Local spin density functional investigations of the chemical bonding and magnetism in the CMR pyrochlore compound $Tl_2Mn_2O_7$

S. F. Matar,[a] M. A. Subramanian[b] and J. Etourneau[a]

[a]*Institut de Chimie de la Matière Condensée de Bordeaux—CNRS, Château Brivazac, Avenue du Docteur Schweitzer, F-33608 Pessac Cedex, France*

[b]*Dupont Central Research and Development, Experimental Station, Wilmington, DE 19880–0328, USA*

The electronic and magnetic structures of the ferromagnetic pyrochlore compound $Tl_2Mn_2O_7$, exhibiting colossal magnetoresistance (CMR), are self-consistently calculated within the local spin density functional theory using the augmented spherical wave (ASW) method. The influence of mixing between the different *l*-valence states on the chemical bonding is discussed from the site projected densities of states (DOS) and from the crystal orbital overlap population (COOP). From this a description of the nature of chemical bonding is proposed in relation with the development of the magnetic moment of Mn (2.77 μ_B) which is found in good agreement with experimental results. Besides, from the calculations a new magnetic property of a weakly half-metallic ferromagnet is proposed.

Several perovskite-based lanthanum manganites have been recently investigated for their colossal magnetoresistance (CMR) properties.[1] Additionally, pyrochlore-type compounds $A_2Mn_2O_7$ (A = rare earth, Y, Sc, In, Tl) have been studied for the same purposes[2–5] because they are likely to present different magnetic exchange interactions than in the former class of compounds, *i.e.* super-exchange instead of double-exchange. In this category of compounds the ferromagnetic system $Tl_2Mn_2O_7$ presents the interesting feature of a much larger conductivity than the other members where A is a rare earth, Y, Sc or In.[6] This basically arises from the contribution of Tl(6s) states to the density of states (DOS) at the Fermi level (E_F) as schematically proposed.[7] For the purpose of further assessing this observation as well as for obtaining the electronic and magnetic structures of $Tl_2Mn_2O_7$ we presently investigate this system within the local spin density functional theory.

The ASW calculational method

As in our earlier studies of magnetic oxide systems[8–10] we use the augmented spherical wave (ASW) method[11] to calculate the electronic and magnetic properties of $Tl_2Mn_2O_7$. In the limited ASW basis set, the valence partial waves for the different species are as follows: Tl (6s,6p,6d), Mn (4s,4p,3d), O (2s,2p), *i.e.* $l_{max}=2$ for Tl and Mn and $l_{max}=1$ for oxygen (*l* is the secondary quantum number).

The reliability of the ASW method arises from its use of the very successful density functional theory (DFT)[12] which accounts for the ground-state properties of a system (calculations done at 0 K). The electron density is then considered to be the fundamental variable (rather than the much more complicated many-body electron wavefunction). Total energy and all other quantities which can be derived from it are then expressed as functionals, $F[\rho]$, of the ground-state electron density ρ. The effects of exchange and correlation are treated within the local spin density approximation (LSDA) using the parametrization scheme of von Barth and Hedin[13] and Janak.[14] Further the ASW method uses the atomic sphere approximation (ASA). The ASA assumes overlapping spheres centred on the atomic sites; the volume of the atomic spheres has to be equal to the cell volume. Within the spheres the potential has a spherical symmetry. The radial ASWs are constructed using spherical functions of two kinds: Hankel-type, centred within the atomic sphere and Bessel-type extending out of the sphere toward neighbouring sites. The augmentation procedure is necessary to ensure the continuity of the wavefunction, in value and first derivative, at the surface of the atomic sphere.[11] The ASA is unproblematic for closely packed structures like metals and intermetallics but for loosely packed structures such as pyrochlore an artefact is used. This is done by introducing empty spheres (ES) to represent the interstitial space and to avoid an otherwise too large overlap between the actual atomic spheres of Tl, Mn and O. Empty spheres are 'pseudo-atoms' with zero atomic number. They receive charges from the neighbouring atomic species and allow for possible covalency effects within the lattice. Our non-unique choice of the atomic sphere radii was subjected to the following ratios: $r_{Tl}/r_{Mn}=1.17$, $r_{Mn}/r_O=1.04$ and $r_O/r_{ES}=1.02$. Such values allow us to minimize the overlap between the atomic spheres. Other ratios were tested without any change of the obtained results. The Brillouin zone (BZ) integration was carried out for a sufficiently large number of *k* points (110 here) in the irreducible wedge of the first zone of the face-centred cubic Bravais lattice. Self consistency was obtained when no variation of the charge transfers ($\Delta Q<10^{-8}$) and of the total variational energy E_{var} ($\Delta E<10^{-7}$ eV) could be observed upon additional cycles.

Furthermore the chemical bonding features are discussed based on the concept of crystal orbital overlap population (COOP) which was introduced by Hoffmann[15] from the quantum chemistry standpoint (extended Hückel calculations). In short the COOP is based on the expectation values of operators which consist of the non-diagonal elements of the overlap population matrix,

$$c^*_{ni}(\boldsymbol{k})S_{ij}c_{nj}(\boldsymbol{k})=c^*_{ni}(\boldsymbol{k})<\chi_{ki}(\boldsymbol{r})|\chi_{kj}(\boldsymbol{r})>c_{nj}(\boldsymbol{k})$$

where S_{ij} represents an element of the overlap matrix of the basis functions and the $c_{nj}(\boldsymbol{k})$ are the expansion coefficients entering the wavefunction of the *n*th band. Partial COOP coefficients $C_{ij}(E)$ are then obtained by integrating the above expression over the Brillouin zone:

$$C_{ij}(E)=C_{ji}(E)=1/\Omega_{BZ}\Sigma_n\int_{BZ}\mathrm{d}^3\boldsymbol{k}\,\mathrm{Re}\{c^*_{ni}(\boldsymbol{k})S_{ij}c_{nj}(\boldsymbol{k})\}\delta(E-\varepsilon_{n\boldsymbol{k}})$$

(Dirac notation δ) which in a somewhat lax notation is often designated as the overlap-population-weighted DOS. The total COOP are then evaluated as the sum over all non-diagonal elements, *i.e.*

$$C(E)=\Sigma_{ij(i\neq j)}C_{ji}(E)$$

For a detailed description and for significant examples we refer the reader to a recent work of Eyert.[16a] We implemented the COOP in the ASW method[16b] with the objective to extract further information on the chemical bonding. This enabled for the calculation of the COOP within density functional theory.

Crystal structure

$Tl_2Mn_2O_7$ crystallizes in the $Fd3m$ space group with eight formula units per unit cell. The atoms are located at the following positions: Tl (16d), Mn (16c), O (48f with $x=0.3254$) and O′ (8b). The presence of two oxygen sublattices in the pyrochlore structure is a relevant feature which differentiates it from the cubic perovskite one which exhibits only one oxygen sublattice. Fig. 1 shows a projection of the structure which can be visualized as corner-sharing $(MnO)_6$ octahedra. The octahedra form a six-edge ring in the middle of which Tl is situated with two O′ on either side of the ring so that the $(TlO)_8$ polyhedra are formed of 6O and 2O′.[6]

The lattice constant was determined on powder samples at 50 K from neutron diffraction studies: $a=9.8819$ Å, and on a single crystal by X-ray diffraction at 296 K: $a=9.892(7)$ Å.[3] Since 0 K ground-state properties are calculated in the framework of LSDF, we use the low-temperature value throughout. Lastly within the ASA, we introduced ES at the (8a) and (32e) positions.

Calculations and results

Non-spin-polarized (NSP) calculations

Objectives of the NSP calculations. $Tl_2Mn_2O_7$ orders ferromagnetically with zero-field $T_C=142$ K. The magnetization from magnetic measurements in 5T field is 2.74 μ_B and from neutron diffraction refinement 2.5 ± 0.2 μ_B per Mn.[2,3]

However in a first step we performed non-spin polarized (NSP) calculations, *i.e.* we enforced spin degeneracy for all states. From the results of such calculations the chemical bonding can be easily addressed. To the very end this is related to the fact that the spin polarized bands result from the NSP bands by a rigid bands shift. Hence it is well justified to discuss the chemical bonding already from the NSP results. Using the Stoner theory of band ferromagnetism[17] the NSP calculations finally allow prediction of the possible onset of magnetism *via* the density of states (DOS) at the Fermi level.

Results. In our choice of the atomic radii, charge transfer occurs, as chemically expected, from Tl and Mn toward O and the empty spheres. However its magnitude is not significant of any large ionic character leading to, say Mn^{4+}. It needs to be stressed that in the framework of ASW calculations the formal ionicity cannot be obtained although a correct representation of the physical and magnetic properties can be described such as in the ferromagnetic oxide CrO_2.[18,19]

The site projected DOS are shown in Fig. 2 (upper) for Mn and O atoms which predominate the density of states of $Tl_2Mn_2O_7$. They are weighted with the multiplicity of the atoms per formula unit. This explains the relatively large DOS intensity of oxygen. The energy scale along the horizontal axis is taken with reference to E_F. For sake of clarity, it is given in an energy window which does not allow one to observe the low lying O 2s states. The main features are dominated by a continuous block from -8 to -1.5 eV mainly formed by O 2p states then by two peaks dominated by Mn 3d centred at and above E_F respectively. This broad band which includes the lower part of Mn 3d is an indication of the covalency of the chemical bond between Mn and O. There is a large intensity DOS at E_F mainly arising from Mn 3d and to a lesser extent from oxygen states. From this the system is unstable in the non-magnetic state, *i.e.* it will incur further stabilization if the corresponding states split by intra-band polarization. Quantitatively, this involves the Stoner criterion of band ferromagnetism.[17] At 0 K, if the inequality $\boldsymbol{I}.N(E_F)>1$ [$\boldsymbol{I}$: Stoner exchange-correlation integral and $N(E_F)$ the NSP DOS] is obeyed then the relevant band should split giving rise to a magnetic moment. From our calculations for Mn 3d, $\boldsymbol{I}\approx 1.0$ eV and $N(E_F)\approx 6\,eV^{-1}$ so that the product of 6 makes the Stoner criterion largely obeyed.

As expected oxygen does not obey the Stoner criterion. Above E_F, the DOS in the 1.5–4 eV range are dominated by empty Mn 3d states and above 6 eV by O and Tl states.

The character of the manganese–oxygen interaction can be further discussed by examining the COOP for the two different kinds of oxygen atoms. The lower panel of Fig. 2 gives the interaction of manganese atom with neighbouring oxygen atom as well as with the other type of oxygen site. The COOP are plotted with the same energy window as the DOS part to enable comparison. They are dominated by the bonding

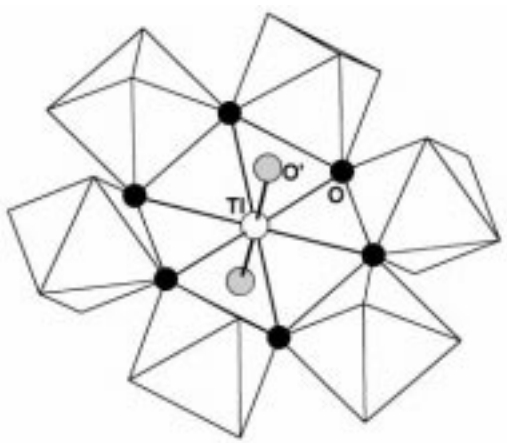

Fig. 1 Partial representation of the crystal structure of $Tl_2Mn_2O_7$

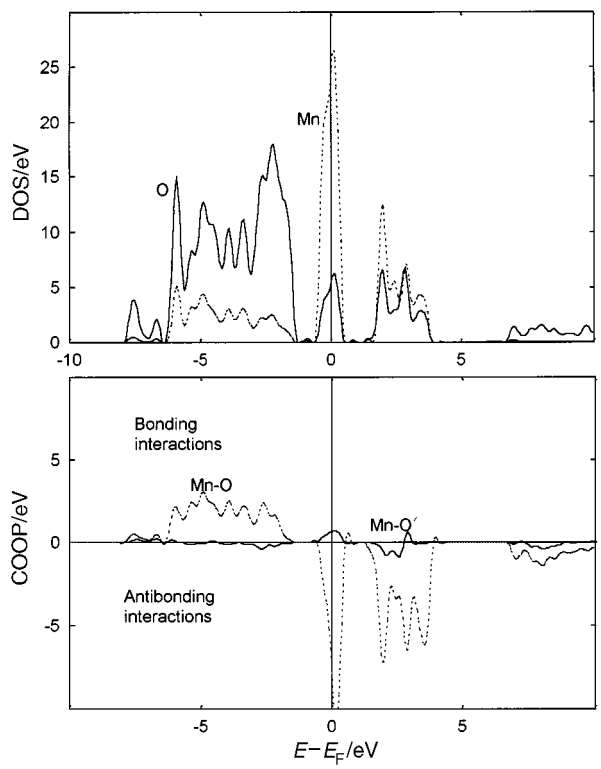

Fig. 2 Non-spin polarized $Tl_2Mn_2O_7$. Upper: site projected DOS of Mn and neighbouring oxygen (O in Fig. 1). Lower: COOP for Mn−O and Mn−O′ interactions.

Mn—O interaction in the valence band, *i.e.* in the range −6 to −1.5 eV. This involves the lower part of the Mn 3d band because these interactions become antibonding for the higher part of Mn 3d at and above E_F. Disregarding relative intensities, it is interesting to note that the skyline of the Mn—O interaction does not follow the DOS in the panel above. This is so for the lower energy part of the massif around −7.5 eV on the one hand and for the higher energy part around −2.5 eV on the other. For the former, there is hardly any Mn—O COOP, because oxygen states are involved in bonding with Tl states. The latter COOP at higher energy corresponds to the large oxygen peak in the upper panel at around −2.5 eV. At this energy there are predominating O···O antibonding interactions not shown here. Likewise at the Fermi level the antibonding Mn—O COOP peak does not involve all the Mn 3d states; as we already discussed in magnetic cubic perovskite systems.[9,10] Thus the largest Mn—O bonding characteristic can be seen around −5 eV. From the very low COOP intensity of Mn–O′ interaction, clearly O′ does not interact with Mn. This follows from the crystal structure (Fig. 1), *i.e.* O′ mainly bonds with Tl. However there is a small bonding contribution at E_F, likely to be the consequence of indirect interactions within the lattice.

In order to elucidate the role of thallium in the DOS, the s and p,d DOS are shown in Fig. 3 (upper). They are clearly dominated by Tl 6s states which show contribution from −8 eV up to E_F. Tl 6s shows larger DOS between −8 and −6.5 eV as well as at E_F than Tl 6p states which are mainly present in the conduction band above 6 eV. Due to their relatively large intensity at E_F, Tl 6s states are likely to contribute to the Fermi surface of the compound and to its conductivity in agreement with ref. 7. Their presence in the conduction band as well, within the same energy range as that of Mn 3d, clearly implies the predominance of covalent bonding in the lattice. Therefore magnetic calculations with two spin populations should reveal spin polarization for the other non-magnetic constituents of the unit cell. This will be accounted for in the following section. Fig. 3 (lower) shows the O′ DOS

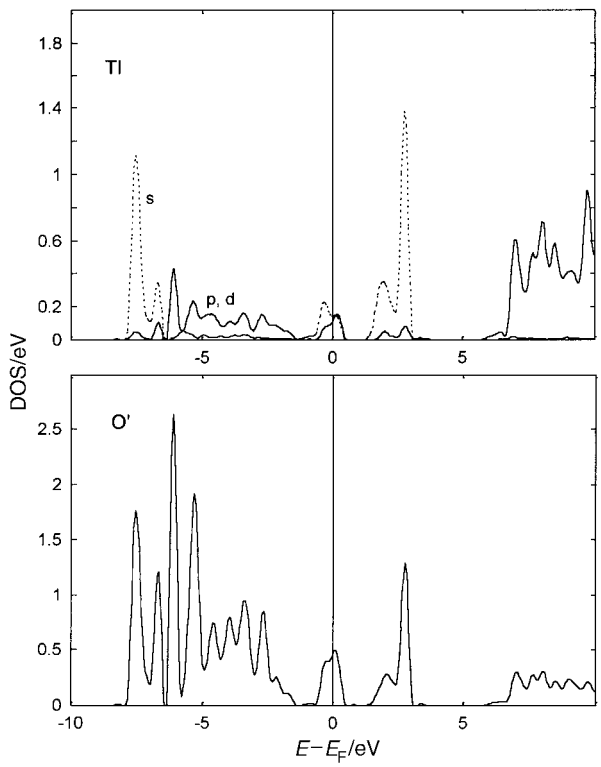

Fig. 3 Non-spin-polarized $Tl_2Mn_2O_7$. Site projected DOS of Tl and oxygen (O′ in Fig. 1).

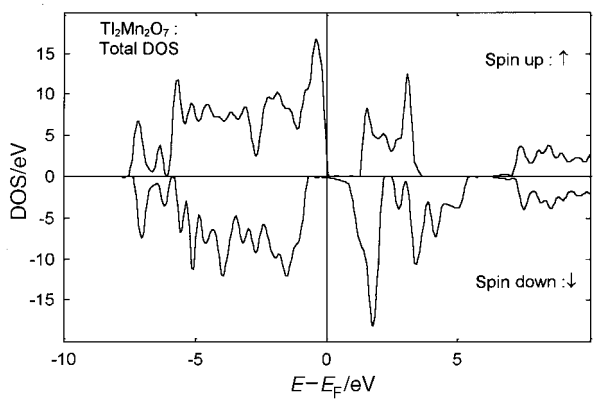

Fig. 4 Density of states (DOS) for ferromagnetic $Tl_2Mn_2O_7$

which closely follow those of Tl thus pointing to the covalency of the Tl—O′ bond. This is especially so for the lower energy part of the valence band around −7.5 eV with the predominance of Tl 6s states as well as for the higher energies around −5 eV where mainly O 2p are present. Interestingly, although still present, the broad valence band is less prominent than in Fig. 2 and rather exhibits atomic-like features meaning that O′ sites are less involved in the covalent bonding within the lattice.

We now turn to spin polarized calculations which are closer to the representation of the properties of the actual physical system.

Spin polarized (SP) calculations

Spin polarized calculations were carried out by initially allowing for two spin occupations, *i.e.* majority (spin up ↑) and minority (spin down ↓) spin directions for all atomic species. Self-consistency was achieved by converging the charges and the magnetic moments for a sufficiently large number of k points. The present calculations, which account for only one magnetic/crystallographic sublattice of Tl, Mn, O and O′ should correctly describe the proper ferromagnetic order. The same number of k points were used and convergence was achieved with the same energy criteria as for the NSP case.

Magnetic moments. From the results the total variational energy of the magnetic configuration is found 0.875 eV per formula unit lower with respect to the NSP one. This stabilization which agrees with the fact that $Tl_2Mn_2O_7$ is a ferromagnet is an expected result because the large $N(E_F)$ values, mainly due to Mn 3d, in the NSP calculations make the non-magnetic configuration unstable with respect to the onset of intra-band spin polarization.

Total magnetization per formula unit is 5.985 μ_B. It arises from a moment of 2.78 μ_B carried by manganese which is in fairly good agreement with experimental investigations, as well as from a polarization of Tl and O states due to the largely covalent interaction in the lattice as shown earlier. Albeit small, the polarization of Tl and O amounts to 0.21 μ_B. The moment of *ca.* 6 μ_B per $Tl_2Mn_2O_7$ could point to Mn^{IV}, *i.e.* a formal $3d^3$ configuration for manganese similar to the 2 μ_B moment for CrO_2 ($3d^2$ configuration for Cr^{IV}) obtained by the same calculational method.[18,19] These features are also in accord with recent investigations of perovskite type manganites by Pickett and Singh[20] and by Singh†.[21]

We shall further illustrate these results by examining the DOS and the band structure.

Density of states and band structure. Fig. 4 shows the DOS of $Tl_2Mn_2O_7$ for majority (↑) and minority (↓) spin directions.

† Ref. 21 was noticed during the course of the submission of this paper.

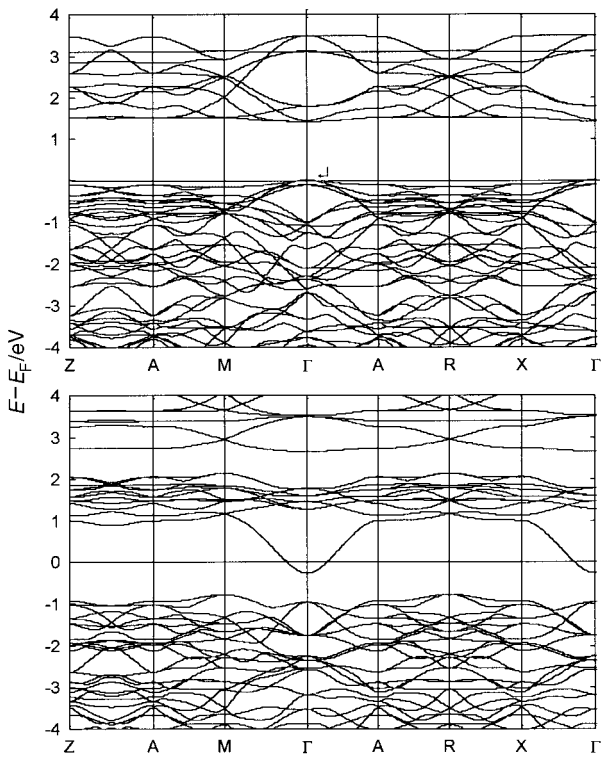

Fig. 5 Band structure of ferromagnetic $Tl_2Mn_2O_7$. Upper: majority spins (↑) ; lower: minority spins (↓).

The relevant feature is that the Fermi level lies in a very low magnitude DOS for both spin directions. The Fermi level crosses the majority spins DOS at a low magnitude leading to an energy gap of nearly 1.5 eV separating the valence band from the conduction band. This is apparent too for the other spin direction but there are low magnitude DOS crossing E_F. This leads to the suggestion that the details can only be observed upon examining the band structure in the close neighbourhood of Fermi level which we show in next paragraph. Spin polarization mainly affects the Mn 3d states whose exchange splitting amounts to *ca.* 3 eV. Less splitting occurs in the energy range −8 to 2 eV where mainly oxygen states are observed. Covalent mixing between the states of the different constituents leads to the presence of Tl as well as O and O′ states in the close neighbourhood of E_F as previously stated in ref. 7. For the purpose of detailing the DOS at E_F, the band structure of ferromagnetic $Tl_2Mn_2O_7$ is shown in Fig. 5. The bands are given in two panels within narrow energy windows showing the valence states for the two spin directions. A general feature is the small dispersion of the bands and their grouping in continuous blocks such as in the energy range −4 to 0 and −4 to −1 eV for the Mn−O valence states for majority and minority spins, respectively. In the conduction band empty d states can be seen in the range 1.5–3.5 for majority spins (↑) and 1–2 eV for minority spins (↓). However there is a larger dispersion for minority spins where a single band can be seen to cross Fermi level at the centre of the Brillouin zone, *i.e.* the Γ point. This feature has its 'image', *i.e.* the corresponding hole, for majority spin bands but it can scarcely be observed (see arrow ↲) because of the very small dispersion of the majority spin bands in the neighbourhood of E_F. Without these features at E_F the compound would be a small-gap semiconductor. This leads to a nearly 100% polarization of (↑) spins and to the closely integer value of the magnetization (*ca.* 6 μ_B). A similar result was obtained for CrO_2[18,19] theoretically announced to be a half-metallic ferromagnet and experimentally verified *a posteriori* by magneto-optical Kerr effect investigations.[22] The major difference between the two oxides lies however in the magnitude of the DOS at Fermi level. Whereas in CrO_2, E_F crosses a large magnitude of Cr 3d(t_{2g} ↑) bands, there is a single band crossed by E_F in $Tl_2Mn_2O_7$. The character of the band is mainly Mn 3d but a contribution of Tl s states gives it a large dispersion at point Γ. The rather different behaviour of the two spin channels could be in relation with the CMR property of $Tl_2Mn_2O_7$. Further experimental investigations should be of great help.

Conclusion

The purpose of the present work was to address the interplay between hybridization leading to the chemical bonding and magnetism in the CMR pyrochlore oxide: $Tl_2Mn_2O_7$. From the analysis of the density of states of the non-magnetic calculations, the role of Mn 3d states in the instability of this magnetic configuation (NSP) toward spin polarization (SP) and the occurrence of a finite density of states from Tl 6s at E_F have been shown.

From spin-polarized calculations, the magnetic moment carried by Mn is found in good agreement with experiment. Furthermore from the SP calculations, a new property of a weakly half-metallic ferromagnet close to a semiconducting one is proposed. This computed result for $Tl_2Mn_2O_7$ should promote investigation of this compound from the point of view of the magneto-optical Kerr effect although its Curie temperature is below room temperature.

References

1 S. Jin, T. H. Tiefel, M. McCormack, R. A. Fastnacht, R. Ramesh and L. H. Chen, *Science*, 1994, **264**, 413.
2 Y. Shimakawa, Y. Kubo and T. Manako, *Nature* (*London*), 1986, **379**, 53 .
3 M. A. Subramanian, B. H. Toby, A. P. Ramirez, W. J. Marshall, A. W. Sleight and G. H. Kwei, *Science*, 1996, **273**, 81.
4 S.-W. Cheong, H. Y. Hwang, B. Batlogg and L. W. Rupp Jr., *Solid State Commun.*, 1996, **98**, 163.
5 M. A. Subramanian, J. E. Greedan, N. P. Raju, A. P. Ramirez and A. W. Sleight, *Proceedings of the ICF7 conference*, Bordeaux, September 1996, 1997, in press.
6 M. A. Subramanian, C. C. Torardi, D. C. Johnson, J. Pannetier and A. W. Sleight, *J. Solid State Chem.*, 1988, **72**, 24.
7 D.-K. Seo, M.-H. Whangbo and M. A. Subramanian, *Solid State Commun.*, 1997, **101**, 417.
8 G. Demazeau, B. Siberchicot, S. F. Matar, C. Gayet and A. Largeteau, *J. Appl. Phys.*, 1994, **75**, 8.
9 S. F. Matar, G. Demazeau, P. Mohn, V. Eyert and S. Najm, *Eur. J. Solid State Inorg. Chem.*, 1994, **31**, 615.
10 S. F. Matar, A. Villesuzanne and M. Uhl, *J. Mater. Chem.*, 1996, **6**, 1785.
11 A. R. Williams, J. Kübler and C. D. Gelatt Jr., *Phys. Rev. B*, 1979, **19**, 6094.
12 W. Kohn and P. Vashishta, in *Theory of the Inhomogeneous Electron Gas.*, ed. S. Lundquist and N. H. March, Plenum, New York, 1983, pp. 79–147.
13 J. von Barth and D. Hedin, *J. Phys. C*, 1972, **5**, 1629.
14 J. F. Janak. *Solid State Commun.* 1978, **25**, 53.
15 R. Hoffmann and C. Zheng, *J. Phys. Chem.*, 1985, **89**, 4175.
16 (*a*) V. Eyert, *Electronic Structure Calculations for Crystalline Materials* in *Density Functional Methods: Applications in Chemistry and Materials Science*, ed. M. Springborg, Wiley, Chichester, 1997; (*b*) V. Eyert and S. F. Matar, 1997, to be published.
17 E. C. Stoner, *Proc. R. Soc. London*, 1938, **165**, 372.
18 K. Schwarz, *J. Phys. F: Met. Phys.*, 1986, **16**, L211.
19 S. F. Matar, G. Demazeau, J. Sticht, V. Eyert and J. Kübler, *J. Phys. I France*, 1992, **2**, 315.
20 W. E. Pickett and D. J. Singh, *Phys. Rev. B*, 1996, **53**, 1146.
21 D. J. Singh, *Phys. Rev. B*, 1997, **55**, 313.
22 H. Brändle, D. Weller, J. C. Scott, P. M. Oppeneer and G. Güntherodt. *Int. J. Mod. Phys. B*, 1993, **7**, 345.

Paper 7/00530J; *Received* 23*rd January*, 1997